Galaxy Zoo 1: data release of morphological classifications for nearly 900 000 galaxies[★]

Chris Lintott,[1,2]† Kevin Schawinski,[3,4]†‡ Steven Bamford,[5] Anže Slosar,[6] Kate Land,[1] Daniel Thomas,[7] Edd Edmondson,[7] Karen Masters,[7] Robert C. Nichol,[7] M. Jordan Raddick,[8] Alex Szalay,[8] Dan Andreescu,[9] Phil Murray[10] and Jan Vandenberg[8]

[1]*Oxford Astrophysics, Denys Wilkinson Building, Keble Road, Oxford OX1 3RH*
[2]*Adler Planetarium, 1300 S. Lake Shore Drive, Chicago, IL 60605, USA*
[3]*Department of Physics, Yale University, New Haven, CT 06511, USA*
[4]*Yale Center for Astronomy and Astrophysics, Yale University, PO Box 208121, New Haven, CT 06520, USA*
[5]*Centre for Astronomy & Particle Theory, University of Nottingham, University Park, Nottingham NG7 2RD*
[6]*Brookhaven National Laboratory, Upton, NY 11973, USA*
[7]*Institute of Cosmology and Gravitation, University of Portsmouth, Dennis Sciama Building, Burnaby Road, Portsmouth PO1 3FX*
[8]*Department of Physics and Astronomy, Johns Hopkins University, 3400 N. Charles St., Baltimore, MD 21218, USA*
[9]*LinkLab, 4506 Graystone Ave., Bronx, NY 10471, USA*
[10]*Fingerprint Digital Media, 9 Victoria Close, Newtownards, Co. Down BT23 7GY*

ABSTRACT

Morphology is a powerful indicator of a galaxy's dynamical and merger history. It is strongly correlated with many physical parameters, including mass, star formation history and the distribution of mass. The Galaxy Zoo project collected simple morphological classifications of nearly 900 000 galaxies drawn from the Sloan Digital Sky Survey, contributed by hundreds of thousands of volunteers. This large number of classifications allows us to exclude classifier error, and measure the influence of subtle biases inherent in morphological classification. This paper presents the data collected by the project, alongside measures of classification accuracy and bias. The data are now publicly available and full catalogues can be downloaded in electronic format from http://data.galaxyzoo.org.

Key words: methods: data analysis – galaxies: elliptical and lenticular, cD – galaxies: general – galaxies: spiral.

1 INTRODUCTION

The aim of the Galaxy Zoo project was to provide visual morphologies for nearly one million galaxies from the Sloan Digital Sky Survey (York et al. 2000), including the whole Main Galaxy Sample (MGS) (Strauss et al. 2002). Separating galaxies into categories based on their morphology (the visual appearance or shape) has been standard practice since it was first systematically applied by Hubble (1936). These morphological categories are broadly correlated with other, physical parameters, such as the star formation rate and history, the gas fraction and dynamical state of the system (Roberts & Haynes 1994); understanding these correlations and studying the cases where they do not apply is critical to our understanding of

the formation and evolution of the galaxy population. It is tempting to identify the morphological distinctions with the clear colour bimodality in the population of galaxies visible in data from modern surveys (e.g. Strateva et al. 2001), but extremely large sets of classified galaxies are necessary before this hypothesis can be tested. For most of the 20th century, morphological catalogues were compiled by individuals or small teams of astronomers (e.g. Sandage 1961; de Vaucouleurs et al. 1991), but modern surveys containing many hundreds of thousands of galaxies make this approach impractical.

Attempts to solve this problem have taken one of three approaches. The first is to use physical parameters, such as colour, concentration index, spectral features, surface brightness profile, structual features, spectral energy distribution (Kinney et al. 1996) or some combination of these as a proxy for morphology (e.g. Abraham, van den Bergh & Nair 2003; Conselice 2006). As no proxy is an exact substitute for true visual morphology, the introduction of each of these variables results in an unknown and potentially unquantifiable bias in the resulting sample of galaxies. Although morphological labels are often used for the resulting catalogues,

---

usually after comparison with a small number of expert classifications, each of these techniques produces catalogues that cannot entirely reproduce true morphological selection. For example, Schawinski et al. (2007) showed that the proportion of elliptical galaxies with recent star formation or nuclear activity was significantly higher in a sample classified by eye than in samples assembled using proxies for morphology. This reflects the fact that proxy quantities such as colour do not directly probe the dynamical state of the system that controls the morphology.

The second strategy was applied by Lahav et al. (1995) and then further developed by Ball et al. (2004) amongst others. The aim was to develop automatic classification routines, typically neural networks, to the point that they can replace the need for human classifications. While successful in classifying the majority of galaxies, a major problem is that due to both the use of proxies for morphology as input and the inherent complexity of the network, it is not easy to predict or understand the bias in the resulting classifications. As a result these automatic classifiers have not been widely adopted.

The third approach is to attempt to expand the reach of visual classifications. Previous professional attempts (Fukugita et al. 2007; Nair & Abraham 2010) have been necessarily limited by the extraordinary effort required to classify even relatively small subsets of the SDSS; the largest, MOSES (Schawinski et al. 2007), included basic classifications of only 50 000 galaxies at redshifts between 0.05 and 0.1, and with $r < 16.8$ (∼5.5 per cent of the SDSS). The results presented in this paper, which expands on our first description of the Galaxy Zoo project and its results (Lintott et al. 2008), provide estimates of the visual morphology of the entire SDSS main galaxy sample. Having produced a catalogue of visual morphologies, we can use the other measured parameters, including colour, to investigate the galaxy population.

Galaxy Zoo is possible because of the involvement of hundreds of thousands of volunteer 'citizen scientists'. The involvement of non-professionals in astronomical science has a long and distinguished history. From the early contributions of observers to modern discoveries of supernovæ and follow-up of candidate extrasolar planets (e.g. Barbieri et al. 2007), astronomers have often depended on volunteers. The Galaxy Zoo project expands the role of non-professionals in astrophysics from data collection to include data analysis, a technique that was first successfully employed in astronomy or astrophysics by the Stardust@Home project (Westphal et al. 2006; Mendez et al. 2008). Its usefulness is demonstrated not only by the catalogue presented here, but also by the serendipitous discovery of unusual objects and classes of object discussed elsewhere (e.g. Cardamone et al. 2009; Lintott et al. 2009).

2 SAMPLE SELECTION AND WEB SITE OPERATION

The images of galaxies presented for classification by Galaxy Zoo were drawn from the Sloan Digital Sky Survey, a survey of a large part of the northern sky providing photometry in five filters (Fukugita et al. 1996; Smith et al. 2002) and covering ∼26 per cent of the sky. Data Release 6 (DR6, Adelman-McCarthy et al. 2008) was used for the initial selection of candidates. We include the Main Galaxy Sample (MGS) of Strauss et al. (2002) which includes all extended objects with Petrosian magnitude $r < 17.77$, a total of 738 175 galaxies including those for which spectra were not available at the time of the DR6 release. In order to be as inclusive as possible, 155 037 objects which had been included in the SDSS spectroscopic survey (for various reasons, including meeting criteria intended to select for luminous red galaxies, quasars and other

Table 1. Galaxy Zoo classification categories showing schematic symbols as used on the site.

Class	Button	Description
1	⬬	Elliptical galaxy
2	⟳	Clockwise/Z-wise spiral galaxy
3	⟲	Anti-clockwise/S-wise spiral galaxy
4	✦	Spiral galaxy other (e.g. edge on
5	✦	Star or Don't Know (e.g. artefact)
6	⌒	Merger

Figure 1. Main analysis page from the Galaxy Zoo web site.

unusual objects) and subsequently classified as a galaxy due to their spectral properties were added, making a total of 893 212 objects.

Composite images of these objects in the g, r and i bands were provided by the ImgCutout web service (Nieto-Santistebán, Szalay & Gray 2004) on the SDSS SkyServer web site (Szalay et al. 2002) and then shown to visitors to the Galaxy Zoo web site,[1] who were then asked to classify the galaxy into one of the six categories shown in Table 1. Distinguishing clockwise and anticlockwise spirals was not only useful in its own right, but also allowed Masters et al. (2010b) to ensure that their sample of red spirals genuinely included only spirals and not edge-on discs or possible S0 galaxies; spiral arms must have been seen by a majority of classifiers to record significant evidence for either a clockwise or an anticlockwise spin. The size of the image of each galaxy was chosen so that the scale was $0.024R_{\rm p}$ arcsec per pixel, where $R_{\rm p}$ is the Petrosian radius for the system. The images were 423 pixels ($\approx 10R_{\rm p}$ for a typical system) on each side. The interface is shown in Fig. 1. The web site was launched on 2007 July 11, and full details of its operation are given in Lintott et al. (2008).

2.1 Data reduction

The data reduction required to turn clicks provided via a web site into a scientific catalogue is substantial. As well as comparing Galaxy Zoo with existing professional catalogues, Lintott et al. (2008) explored the possibility of weighting users according to how often they agreed with the majority, but found little change to the resulting classifications. Requirements for 80 and 95 per cent

---

[1] The original Galaxy Zoo web site is maintained and archived at http://zoo1.galaxyzoo.org

agreement amongst users were then used to define 'clean' and 'superclean' samples, respectively. This approach, while suitable for some purposes, has proved to be inadequate for others. Darg et al. (2010a), in their study of merging galaxies, found that all galaxies with a fraction of 40 per cent or more of their vote in the 'merger' category were, in fact, true mergers. This result suggests that the application of a single critical threshold to all classifications is oversimplistic. The catalogue presented in this paper therefore includes the fraction of clicks in each category for all galaxies, rather than just those in the 'clean' or 'superclean' samples. Users of the data set presented here are, however, recommended to use cuts of 0.8 or 0.95 in the first instance to ensure where possible that results are comparable with earlier results.

In using the Galaxy Zoo morphologies, it is important to consider the population of galaxies which are unclassified according to the criterion used to assign individual galaxies to a population. It is obviously possible to derive a classification for every galaxy by simply assigning it to the category with the greatest fraction of the vote (which we refer to as the *greater* criterion); a galaxy with 51 per cent of the vote in the elliptical category would, in this system, be considered an elliptical. For more stringent thresholds (e.g. *clean*, where a galaxy would require at least 80 per cent of the vote to be assigned a classification) then unclassified galaxies may form a majority of the sample. In order to evaluate the effect of this feature of the data, we determine the fraction of unclassified galaxies as a function of magnitude and size.

In an effort to quantify the effect of other potential biases in the classification process, mirrored and grey-scale images were introduced to the site from 2007 November 28. The grey-scale images were not single filter images, but in order to minimize the effect of apparent changes in morphology caused by viewing the galaxy in different wavelengths were instead produced from the *gri* colour images provided by the SDSS pipeline. A subsample of the main catalogue sample was used, comprising the *superclean* sample as of 2007 September 4 (i.e. all galaxies with an agreement of more than 95 per cent on that date) and a random sampling of 5 per cent of the rest of the sample, comprising 91 303 images in total. A list of galaxies included in this bias study sample is given in Section 4.

The results of this bias study were discussed in Lintott et al. (2008) and Land et al. (2008). Significant but small biases in spin direction and colour were found, with anticlockwise spiral classifications favoured over clockwise, and the grey-scale images were more likely to be classified as elliptical than their colour counterparts.

Although these biases were small, the effect of studying them was relatively large. Any study of the behaviour of human classifiers is likely to encounter a phenomenon known as the Hawthorne effect (Mayo 1933), the risk of changing the behaviour of those taking part in a study simply by carrying out the study itself. A change in classifier behaviour was indeed observed, with users being slightly more careful in their classifications during the bias study and thus classifying fewer galaxies as spiral. The effect is small (∼3 per cent fewer votes were received in the spiral categories) but significant. Rather than just combining classifications for each of the galaxies included in the bias study, therefore, we present the data from before and then during the study separately.

3 PROPERTIES OF THE DATA

3.1 Quantifying bias

Bamford et al. (2009) carry out a more detailed analysis of the Galaxy Zoo data, initially motivated by the desire to determine the

relationship between morphology and the local density of galaxies. The technique used recognizes that although small, faint or distant galaxies will likely appear as ellipticals and therefore will be classified as such with a high degree of agreement, many of these systems are likely to be spirals whose arms are not distinctly visible in the SDSS images. By assuming that the morphological fraction within bins of fixed galaxy size and luminosity does not evolve over the depth of the SDSS, it is possible to statistically estimate the bias affecting the morphological classifications for galaxies of known luminosity, size and distance. It is important to note that this bias does not arise from the involvement of volunteers in the classification process, but from the inherent limitations of the survey data.

The method only deals with removing the bias relative to the least biased data (i.e. that from nearby systems) and so there may be a remaining, unquantified bias, for example due to bias in human pattern recognition abilities. The bias correction will also reduce the impact of any true redshift evolution from the sample (although only that evolution which affects the morphological mix of the population at a given absolute magnitude and physical size).

The effect of this bias on a final catalogue depends on how the raw Galaxy Zoo classifications are treated. As an example, if a simple majority of the vote is used to classify galaxies then ∼13.5 per cent of galaxies are in absolute magnitude–size bins where approximately no bias correction is necessary, and ∼20 per cent are in bins which have approximately no misclassified galaxies. Conversely, ∼6 per cent of galaxies are in bins where the bias correction changes the classifications for more than half of the objects. In contrast, if the *clean* criterion is used then a much larger fraction, over 70 per cent, of galaxies are in absolute magnitude size bins for which no objects are misclassified due to this bias. The price of applying a more stringent criterion for classification is thus a large fraction of objects which do not meet the *clean* criteria and thus have 'uncertain' classifications.

As determining the bias correction requires a redshift, debiased results are only available for objects which were spectroscopically observed by SDSS, a subset of the whole Galaxy Zoo sample. The determination also requires a well-defined, homogeneous sample and is therefore limited to MGS objects with reliable *r*-band photometry, redshifts in the range of 0.001–0.25 and absolute magnitudes and sizes that are not extreme outliers from the normal galaxy distribution. Bamford et al. (2009) used DR6 of the SDSS which only provided spectroscopic coverage for 82 per cent of the survey area. With the availability of SDSS Data Release 7 (Abazajian et al. 2009), the spectroscopic coverage has risen. As a result, the number of objects with redshifts has increased from 677 515 (76 per cent) to 781 842 (88 per cent). Considering just the Main Galaxy Sample, the total number of objects in Galaxy Zoo is 738 173, of which 679 721 (92 per cent) have redshifts in DR7, up from 575 398 (78 per cent) in DR6. In calculating the classification bias corrections we have thus supplemented our previous DR6 catalogue with additional redshifts from DR7, significantly increasing the fraction of the sample for which we can provide these corrections.

As described in appendix A of Bamford et al. (2009), we first divide the sample into bins of similar luminosity, physical size and redshift. We then find for each point in luminosity–size space the lowest-redshift bin containing at least 30 galaxies, and assume that this bin represents the 'true' early type to spiral ratio. In an attempt to keep this baseline estimate unbiased, we only consider bins well away from the magnitude, size and surface brightness limits of the sample.

Having obtained an approximation to the low-redshift early type to spiral ratio as a function of both luminosity and size, we fit an

appropriate smooth function to the result. Equation (A1) in Bamford et al. gives the fit

$$\left\langle \frac{n_{el}}{n_{sp}} \right\rangle_{base} = \frac{p_1}{1 + \exp\left(\frac{s_1(R_{50}) - M_r}{s_2(R_{50})}\right)} + p_2, \qquad (1)$$

where

$$s_1(R_{50}) = q_1^{-(q_2 + q_3 R_{50}^{q_4})} + q_5$$

and

$$s_2(R_{50}) = r_1 + r_2[s_1(R_{50}) - q_5]. \qquad (2)$$

By considering the difference between this baseline early type to spiral ratio and that measured for a given bin of absolute magnitude, physical size and redshift, we can estimate the correction, C, required for any particular galaxy as

$$C(M_r, R_{50}, z) = \log\left(\frac{\langle n_{el}/n_{sp}\rangle_{raw}}{\langle n_{el}/n_{sp}\rangle_{base}}\right), \qquad (3)$$

where angular brackets indicate averages over bins of (M_r, R_{50}, z).

Individual vote shares (type likelihoods) for each galaxy are adjusted as

$$p_{el,adj} = \frac{1}{1/\left(\left(\frac{p_{el}}{p_{sp}}\right)_{adj} + \frac{p_x}{p_{el}} + 1\right)},$$

$$p_{sp,adj} = \frac{1}{\left(\frac{p_{el}}{p_{sp}}\right)_{adj} + \frac{p_x}{p_{sp}} + 1}, \qquad (4)$$

where

$$\left(\frac{p_{el}}{p_{sp}}\right)_{adj} = \left(\frac{p_{el}}{p_{sp}}\right)_{raw} \Big/ 10^{C(M_r, R_{50}, z)}, \qquad (5)$$

and $p_x = 1 - p_{el} - p_{sp}$.

Fig. 2 illustrates the effect of the bias, and the result of adopting the measured correction, as a function of redshift, apparent magnitude and apparent size, for three bins of absolute magnitude and physical size. The overall result of applying the correction is to lower the probability that a given galaxy will be classified as early type and increase the chance that it will be classified as spiral. The effect is largest around the median SDSS redshift, and for faint, small galaxies; bright, large, low-redshift galaxies need only a small correction, whereas at the highest redshifts only the most luminous galaxies pass the sample selection criteria, most of which are indeed early types.

3.2 Measures of confidence

To assist users of the Galaxy Zoo data set in evaluating the morphological classifications they obtain, both individually and for larger samples, we have calculated a number of relevant statistics. These were derived from the bias correction procedure described above and thus reflect only the sensitivity of the classification to the bias described in the previous section. They do not take into account other systematic biases that may exist in the data set (see Lintott et al. 2008 for a comparison of the Galaxy Zoo classifications with other catalogues of visual morphology).

A first indicator of the quality of an individual morphology is the difference between its raw and debiased likelihoods, Δp. The bias corrections are inherently uncertain, especially when applied to individual galaxies rather than to large samples, but the size of the bias correction is an indication of the uncertainty in the galaxy's type.

To remove the individual uncertainties on our confidence measures, for each galaxy we calculate values computed from a 'bin' of galaxies with similar redshift, absolute magnitude and physical size, corresponding to the same binning used in quantifying the bias correction. We therefore provide the mean and standard deviation of Δp in each galaxy's bin, $\langle \Delta p \rangle$ and $\sigma_{\Delta p}$, respectively.

A confidence measure of perhaps more practical use is an estimate of the probability that a given galaxy may have been classified as an elliptical when it is in reality a spiral. We thus calculate the fraction of objects within a given galaxy's bin that are classified as elliptical using the raw data but as spiral when the effect of the bias correction is taken into account. This fraction of misclassified galaxies, $f_{misclass}$, depends strongly on the threshold used in the analysis to define 'spiral' or 'elliptical', being highest when the *greater* condition is used (i.e. when a galaxy is classified as an elliptical when $p_{el} > p_{sp}$) and smaller when more stringent classifications are used. However, the cost of using a more stringent classification threshold is that an increasing fraction of galaxies are unclassifiable, i.e. they do not meet the criteria for any of the classifications and are thus 'uncertain'. We quantify this by measuring the fraction of unclassified galaxies, $f_{unclass}$, in the same bin of redshift, magnitude and size as the particular galaxy in question.

The distribution of these quantities amongst the Galaxy Zoo sample are shown in Fig. 3 (for the *greater* criterion) and Fig. 4 (for *clean*). Note that weighting the results to favour those users who tend to agree with the majority makes little difference compared with the effect of changing the classification threshold.

Following earlier Galaxy Zoo papers, a *clean* sample has been defined by requiring 80 per cent of the corrected vote to be in a particular category. However, this choice was somewhat arbitrary, and yet has a significant effect on the number of unclassified and misclassified galaxies. This effect is shown in Fig. 5 for four thresholds: 50 per cent (*greater*), 60 per cent (*cleanish*), 80 per cent (*clean*) and 95 per cent (*superclean*). The mean values of each distribution are indicated with arrows. For example, a threshold of 50 per cent results, by design, in a classification for every galaxy but 19 per cent are misclassified. A threshold of 60 per cent results in 33 per cent of galaxies unclassified and 10 per cent misclassified. A threshold of 80 per cent results in 60 per cent of galaxies unclassified and 3 per cent misclassified, while a threshold of 95 per cent results in no misclassifications but 88 per cent of galaxies unclassified. These figures illustrate the general principle of working with these data; as the threshold is made more stringent, then the fraction of unclassified objects increases while the fraction of misclassified objects decreases.

4 THE CATALOGUE

Table 2 contains the data for all MGS galaxies with measured redshifts in the range $0.001 < z < 0.25$ and u and r photometry in SDSS DR7, excluding those with extreme absolute magnitudes or sizes given by the SDSS pipeline. 667 945 galaxies are included. This table includes the raw votes, the weighted votes in elliptical (E) and combined spiral (CS) categories and flags indicating the inclusion of the galaxy in a *clean*, debiased catalogue. The flags take into account not only the redshift dependence of the spiral/elliptical ratio as described in Section 3.1 but also the redshift dependence of the ratio of spirals to ellipticals in the clean catalogue. This results in larger corrections than would otherwise be necessary. As explained above, bias correction was only possible for MGS galaxies for which SDSS DR7 included spectra,
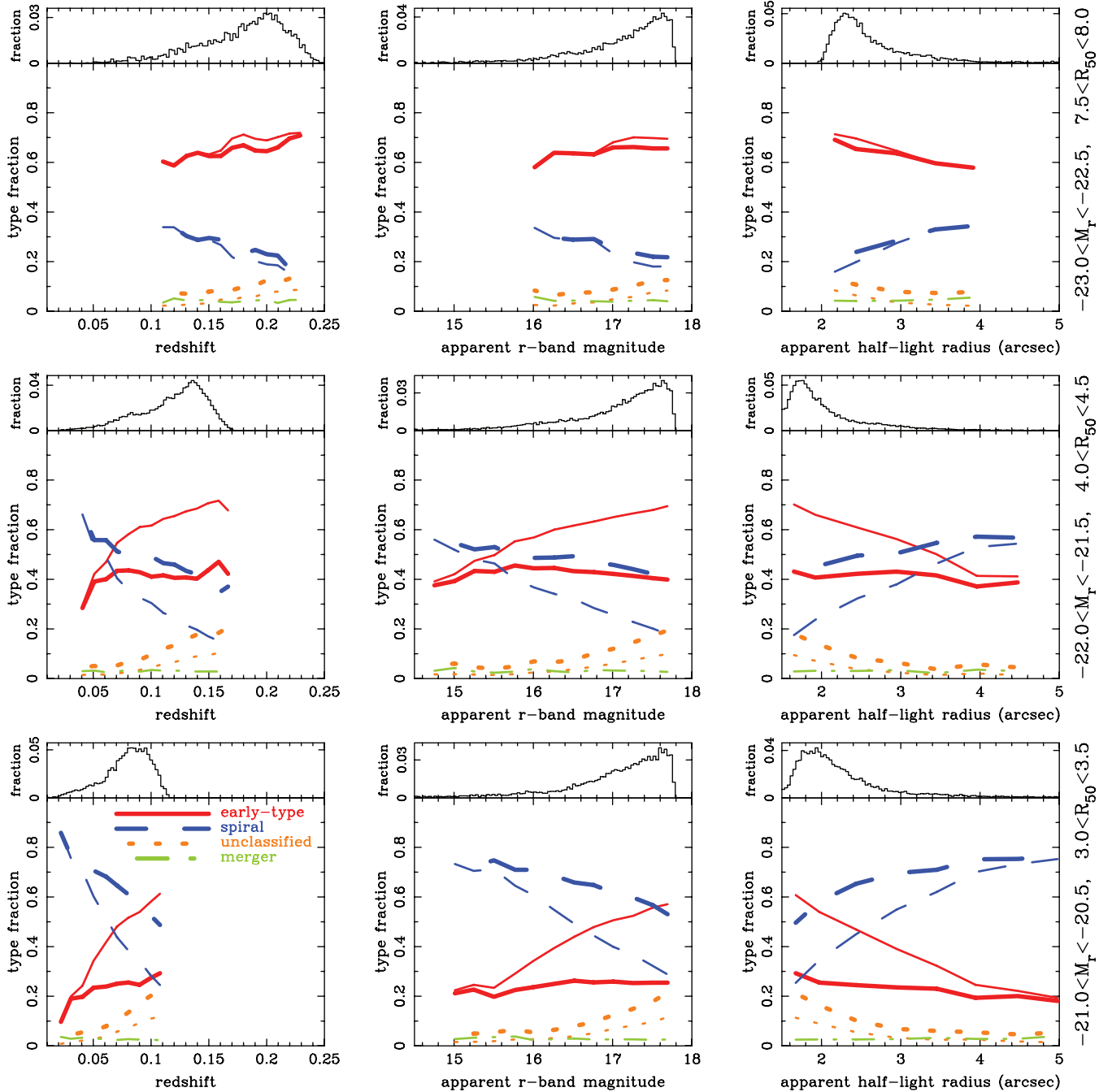
Figure 2. The effect of the bias, and of the result of adopting the measured correction as a function of redshift, apparent magnitude and apparent size. The thin and thick lines correspond to debiased and raw classifications, respectively.

and so Table 3 contains classifications for galaxies included in the Galaxy Zoo sample for which bias corrected morphologies are not available.

As discussed in Section 2.1, while the introduction of mirrored and monochrome images was important in allowing the measurement of human bias, doing so also affected the behaviour of the participants. The measurements obtained during this bias study have thus not been combined with the main data set described above. Table 4 presents the confidence measures discussed in Section 3.2, calculated using absolute magnitude and physical (rather than ap-

parent) size. Tables 5 and 6 give details of the votes assigned to each category for the galaxies which were included in the bias study, as well as a combined vote in Table 7.

4.1 Examples

This paper presents, as a legacy for the community, the entire Galaxy Zoo 1 data set. Users should bear in mind that the objects included in Galaxy Zoo 1 were selected by a combination of criteria (see Section 2), and therefore appropriate additional cuts (in magnitude,
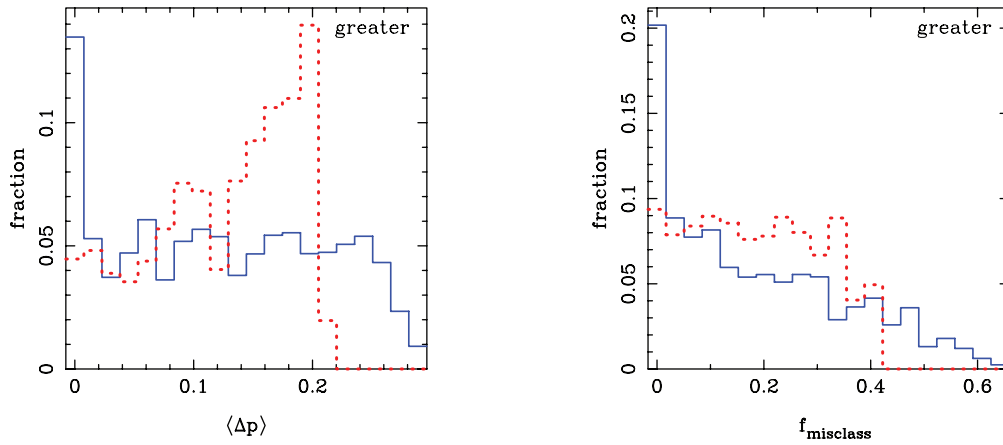
Figure 3. Histograms showing (left) the average bias correction applied to the type-likelihoods (Δp) and (right) the estimated fraction of objects that are misclassified, at the absolute (blue, solid line) and apparent (red, dotted line) magnitude and size of each galaxy in the Galaxy Zoo Main Galaxy Sample. These are calculated using the *greater* classification criteria, as described in the text. For example, note that ∼13.5 per cent of galaxies are in absolute magnitude–size bins where approximately no bias correction is necessary, and ∼20 per cent are in bins which have approximately no misclassified galaxies. Conversely, ∼6 per cent of galaxies are in bins where the bias correction changes the classifications for more than half of the objects.
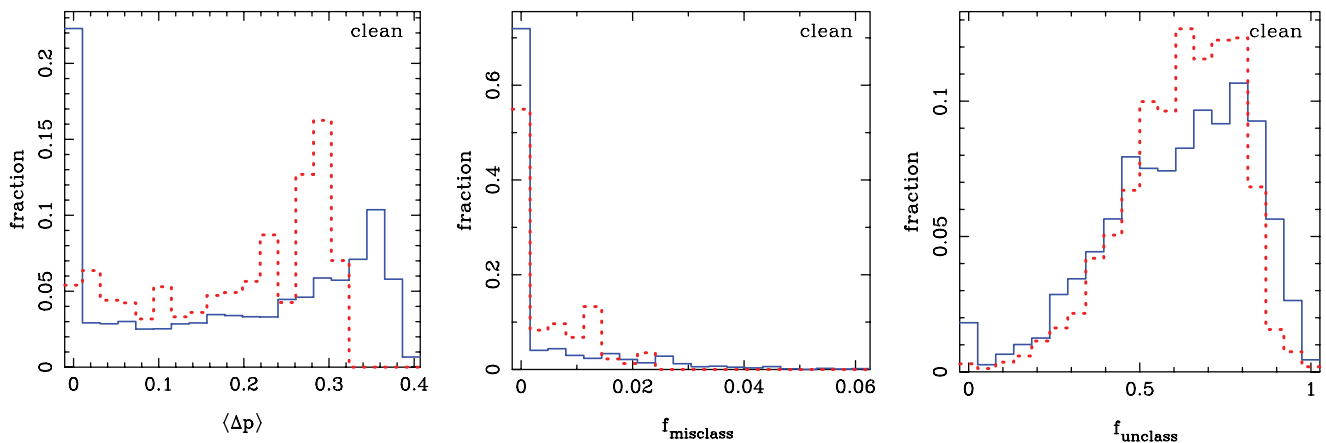
Figure 4. Left and centre as Fig. 3, but for galaxies classified using the *clean* criteria. This figure also includes (right) the fraction of objects that are unclassified by the *clean* criteria, i.e. they have both p_{sp} and $p_{el} < 0.8$. The average corrections are slightly larger for the *clean* versus *greater* criteria, misclassifications are considerably lower, but at the expense of a large fraction of unclassified galaxies. For example, over 70 per cent of galaxies are in absolute magnitude-size bins for which the classification bias results in no objects being misclassified, but roughly two-thirds of galaxies are in absolute magnitude-size bins for which at least half the objects are unclassified.
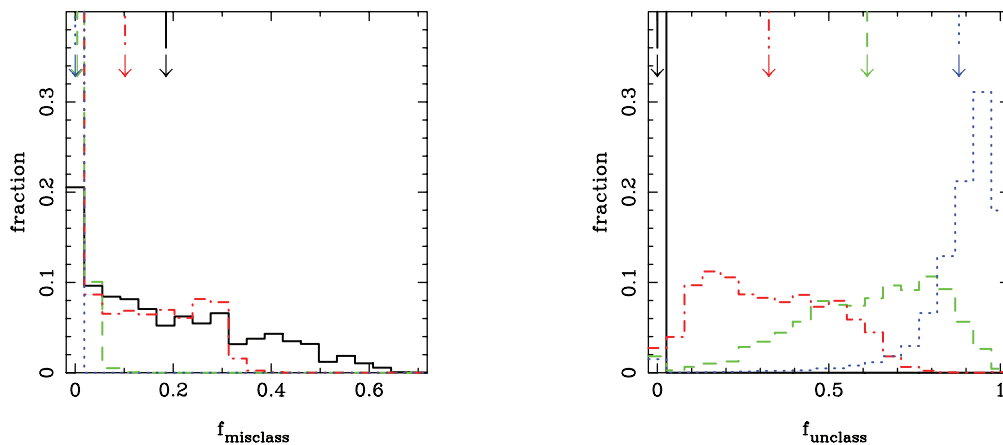
Figure 5. Histograms of (left) fraction misclassified and (right) fraction unclassified, for *greater* (black, solid line), *cleanish* (red, dot–dashed line), *clean* (green, dashed line) and *superclean* (blue, dotted line). The arrows at the top indicate the means of each distribution. One can clearly see that as the classification criteria become more stringent the fraction of misclassified objects decreases, but at the expenses of an increasing fraction of unclassified objects.

Table 2. Classifications of MGS galaxies with spectra.

ObjID[a]	RA	Dec.	N_{vote}[b]	Votes[c] E	CW	ACW	Edge	DK	MG	CS	Debiased votes[d] E	CS	Flags[e] Spiral	Elliptical	Uncertain
587727178986356823	00:00:00.41	−10:22:25.7	59	0.61	0.034	0.0	0.153	0.153	0.051	0.186	0.61	0.186	0	0	1
587727222300741210	00:00:00.74	−09:13:20.2	18	0.611	0.0	0.167	0.222	0.0	0.0	0.389	0.203	0.797	1	0	0
587727225153257596	00:00:01.03	−10:56:48.0	68	0.735	0.029	0.0	0.147	0.074	0.015	0.176	0.432	0.428	0	0	1
587730774962536596	00:00:01.38	+15:30:35.3	52	0.885	0.019	0.0	0.058	0.019	0.019	0.077	0.885	0.077	0	1	0
587731186203885750	00:00:01.55	−00:05:33.3	59	0.712	0.0	0.0	0.22	0.068	0.0	0.22	0.64	0.29	0	0	1
587727180060098638	00:00:01.57	−09:29:40.3	28	0.857	0.0	0.036	0.0	0.107	0.0	0.036	0.83	0.06	0	0	1
587731187277627676	00:00:01.86	+00:43:09.3	38	0.5	0.0	0.053	0.289	0.105	0.053	0.342	0.351	0.473	0	0	1
587727223024189605	00:00:02.00	+15:41:49.8	26	0.423	0.0	0.0	0.577	0.0	0.0	0.577	0.143	0.857	1	0	0
587730775499407375	00:00:02.10	+15:52:54.2	62	0.355	0.016	0.21	0.323	0.0	0.097	0.548	0.355	0.548	0	0	1
587727221950382424	00:00:02.41	+14:49:19.0	31	0.484	0.129	0.065	0.258	0.065	0.0	0.452	0.109	0.789	1	0	0
587730774425665704	00:00:02.58	+15:02:28.3	24	0.583	0.042	0.125	0.167	0.083	0.0	0.333	0.147	0.701	0	0	1
587730773888794751	00:00:02.82	+14:42:55.9	26	0.654	0.077	0.0	0.077	0.192	0.0	0.154	0.621	0.185	0	0	1
588015507658768464	00:00:03.24	−01:06:46.8	57	0.474	0.088	0.0	0.263	0.175	0.0	0.351	0.324	0.48	0	0	1
587727184494485858	00:00:03.33	−10:43:16.0	24	0.125	0.0	0.0	0.875	0.0	0.0	0.875	0.024	0.976	1	0	0
587730773351858407	00:00:03.46	+14:11:53.6	64	0.625	0.016	0.016	0.25	0.078	0.016	0.281	0.245	0.597	0	0	1
587731187277693069	00:00:04.12	+00:45:07.9	30	0.933	0.0	0.033	0.0	0.033	0.0	0.033	0.913	0.054	0	1	0
587727227837612116	00:00:04.18	−08:44:03.0	37	0.73	0.0	0.081	0.135	0.054	0.0	0.216	0.648	0.295	0	0	1
587727225153257606	00:00:04.60	−10:58:34.7	30	0.6	0.0	0.0	0.133	0.233	0.033	0.133	0.368	0.264	0	0	1
587718059969574	00:00:04.60	−08:56:37.6	30	0.167	0.333	0.033	0.467	0.0	0.0	0.833	0.075	0.925	1	0	0
587731187277693072	00:00:04.74	+00:46:54.2	36	0.722	0.083	0.111	0.083	0.0	0.0	0.278	0.606	0.394	0	0	1
587727222300741221	00:00:05.17	−09:13:04.6	66	0.424	0.0	0.03	0.061	0.03	0.455	0.091	0.335	0.133	0	0	1
588015507658768548	00:00:05.54	−01:12:58.9	28	0.179	0.0	0.429	0.321	0.071	0.0	0.75	0.061	0.861	0	0	1
587727221413511423	00:00:05.70	+14:24:44.8	56	0.321	0.036	0.339	0.143	0.125	0.036	0.518	0.069	0.721	0	0	1
587730775499407519	00:00:06.11	+15:52:31.4	58	0.828	0.017	0.0	0.086	0.069	0.0	0.103	0.556	0.326	0	0	1
588015509806252152	00:00:06.67	+00:30:16.8	38	0.711	0.0	0.0	0.132	0.158	0.0	0.132	0.612	0.216	0	0	1
587727221413511425	00:00:06.70	+14:19:58.5	55	0.818	0.036	0.0	0.036	0.109	0.0	0.073	0.818	0.073	0	1	0
588015510343123099	00:00:07.12	+00:51:28.5	47	0.766	0.021	0.043	0.149	0.021	0.0	0.213	0.602	0.373	0	0	1
587727220876440496	00:00:07.35	+13:54:36.6	24	0.833	0.0	0.0	0.125	0.042	0.0	0.125	0.645	0.301	0	0	1
587730775499407506	00:00:07.37	+15:51:19.2	31	0.742	0.0	0.065	0.0	0.097	0.097	0.065	0.513	0.183	0	0	1
587730775499407527	00:00:07.59	+15:54:07.4	50	0.8	0.02	0.0	0.08	0.1	0.0	0.1	0.41	0.362	0	0	1
587730775499407394	00:00:07.62	+15:50:03.2	31	1.0	0.0	0.0	0.0	0.1	0.0	0.0	1.0	0.0	0	1	0

Note. The full version of this table is available from http://data.galaxyzoo.org/. A portion is shown here for guidance regarding its form and content.

[a] SDSS ID. This table includes all galaxies for which spectra are available in SDSS Data Release 7.

[b] Total number of votes for each object.

[c] Fraction of votes for Elliptical (E), ClockWise spirals (CW), AntiClockWise spirals (ACW), Edge-on spirals (Edge), Don't Know (DK), Merger (MG) and Combined Spiral (CS=E+CW+ACW) categories.

[d] Fraction of votes for Elliptical (E) and Combined Spiral (CS=E+CW+ACW) categories following the debiasing procedure described in Section 3.1.

[e] Galaxies flagged as 'elliptical' or 'spiral' require 80 per cent of the vote in that category after the debiasing procedure has been applied; all other galaxies are flagged 'uncertain'.

Table 3. Classifications of additional galaxies.

ObjID[a]	RA	Dec.	N[b]	E	CW	ACW	Votes[c] Edge	DK	MG	CS
5877730774425665700	00:00:01.28	+15:04:40.8	73	0.479	0.0	0.0	0.014	0.479	0.027	0.014
5877727220876640877	00:00:01.86	+14:01:28.2	29	0.655	0.0	0.0	0.0	0.345	0.0	0.0
5877727180060098742	00:00:02.15	−09:31:37.0	30	0.467	0.0	0.033	0.0	0.467	0.033	0.033
588015509806252142	00:00:02.28	+00:37:39.2	29	0.655	0.034	0.034	0.103	0.172	0.0	0.172
5877731187277627683	00:00:02.96	+00:43:04.8	24	0.583	0.0	0.083	0.167	0.125	0.042	0.25
5877731186203951111	00:00:04.44	−00:05:00.1	30	0.967	0.0	0.0	0.033	0.0	0.0	0.033
5877730775499407505	00:00:04.96	+15:51:15.3	45	0.667	0.0	0.044	0.178	0.044	0.067	0.222
5877730774962536621	00:00:05.96	+15:25:47.6	25	0.8	0.0	0.08	0.0	0.0	0.12	0.08
5877730775499407504	00:00:07.22	+15:51:14.2	39	0.59	0.0	0.026	0.026	0.051	0.308	0.051
5877730773888794648	00:00:07.73	+14:39:55.9	28	0.679	0.0	0.036	0.071	0.107	0.107	0.107
5877727225690128558	00:00:08.42	−10:28:23.6	43	0.512	0.023	0.0	0.442	0.023	0.0	0.465
5877727222487318704	00:00:08.83	+15:18:38.3	31	0.419	0.161	0.065	0.323	0.032	0.0	0.548
5877727220876705929	00:00:09.64	+14:05:42.8	25	0.28	0.04	0.04	0.36	0.28	0.0	0.44
5877727225690128563	00:00:11.29	−10:27:41.5	32	0.562	0.0	0.156	0.25	0.031	0.0	0.406
5877727220876705935	00:00:11.92	+14:05:24.0	31	0.258	0.032	0.0	0.0	0.097	0.613	0.032
5877731187814563978	00:00:11.97	+01:07:18.5	30	0.033	0.933	0.0	0.0	0.033	0.0	0.933
5877730773351923943	00:00:13.06	+14:13:18.0	31	0.903	0.032	0.0	0.065	0.0	0.0	0.097
5877727177912615045	00:00:13.11	−11:12:01.0	31	0.806	0.0	0.0	0.097	0.097	0.0	0.097
5877730775499407560	00:00:14.32	+15:52:16.7	29	0.448	0.379	0.0	0.103	0.069	0.0	0.483
5877727179523227783	00:00:15.54	−09:47:55.5	33	0.424	0.061	0.0	0.273	0.182	0.061	0.333
5880155087320510387	00:00:16.12	−00:13:58.4	22	0.545	0.0	0.182	0.091	0.182	0.0	0.273
588015508195639455	00:00:16.19	−00:38:54.9	36	0.556	0.028	0.0	0.167	0.25	0.0	0.194
58777225153323052	00:00:17.96	−10:53:39.8	54	0.556	0.056	0.056	0.167	0.148	0.019	0.278
588015508195639399	00:00:18.69	−00:39:06.6	60	0.3	0.0	0.05	0.467	0.133	0.05	0.517
5877727179523227873	00:00:20.63	−09:48:34.5	52	0.538	0.0	0.0	0.058	0.115	0.288	0.058
5877730774425665840	00:00:21.04	+15:06:08.0	61	0.705	0.0	0.016	0.049	0.23	0.0	0.066
5877730773351923979	00:00:21.19	+14:10:53.7	33	0.212	0.0	0.0	0.152	0.061	0.576	0.152
5877730774425665839	00:00:21.73	+15:06:11.8	44	0.818	0.0	0.045	0.0	0.136	0.0	0.045
5877727226763935920	00:00:22.65	−09:38:18.6	52	0.327	0.115	0.115	0.365	0.077	0.0	0.596
588015507658768569	00:00:24.16	−01:13:20.7	24	0.833	0.0	0.0	0.042	0.083	0.042	0.042
588015507658768511	00:00:24.17	−01:14:44.9	32	0.875	0.031	0.031	0.031	0.031	0.0	0.094
5877727226227064993	00:00:25.55	−09:57:53.0	64	0.719	0.016	0.0	0.109	0.156	0.0	0.125
5877727223024189787	00:00:25.61	+15:41:28.2	33	0.879	0.0	0.03	0.03	0.061	0.0	0.061

Note. The full version of this table is available from http://data.galaxyzoo.org/. A portion is shown here for guidance regarding its form and content.
[a]SDSS ID. This table includes all objects in the Galaxy Zoo sample for which spectra are not included in SDSS Data Release 7.
[b]Total number of votes for each object.
[c]Vote fractions for each category, as defined in the comments for Table 2.

redshift, etc.) should be made to produce a well-defined sample appropriate to any particular study.

Most users of this data will have specific requirements which fall into one of a few categories. For example, one may require a small number of spiral or elliptical galaxies, perhaps for an observing proposal. In this situation, we suggest using a subset of the galaxies which we have flagged as belonging to the relevant category according to the *clean* criterion incorporating the bias correction (Table 2).

The data in Table 4 will then allow the user to estimate the fraction of the derived sample which are misclassified due to inherent classification bias (i.e. the inability to detect spiral arms in faint or small systems). The certainty of the individual classifications can be improved by using a higher threshold (e.g. requiring 95 per cent agreement amongst classifiers) or by selecting nearby, bright and/or large galaxies.

This procedure will suffice for many studies, but one should always consider the properties of the objects with 'uncertain' classifications where these may potentially affect the result. This will be the case for many statistical studies. In such circumstances, it may be preferable to have an estimate of the morphology of all systems, rather than leaving a large number unclassified. In this case, the morphological type likelihoods from Table 2 (ideally the debiased quantities) may be used directly, or a simple majority vote can be applied.

Finally, if the small effect of the change in behaviour associated with the bias study can be ignored, and no bias correction is required, a greater number of votes for ~250 000 systems can be obtained from Table 7.

5 CONCLUSIONS

This paper presents the results of Galaxy Zoo 1, which used the World Wide Web to recruit a large community of volunteers to provide morphological classifications of galaxies drawn from the Sloan Digital Sky Survey. Such morphological classifications are useful indicators of a galaxy's dynamical state and are correlated with many other physical parameters.

The data presented here have already produced several interesting results. Much of this work, published elsewhere (eg Land et al. 2008; Bamford et al. 2009; Schawinski et al. 2009; Masters 2010a) was only possible because of the large number of morphological classifications provided by the project. The clockwise/anticlockwise classifications of the spiral galaxies have been used to show that (as

Table 4. Measures of confidence.

				clean			greater		
ObjID	RA	Dec.	$f_{unclass}$	$f_{misclass}$	$\langle \Delta p \rangle$	$\sigma_{\Delta p}$	$f_{misclass}$	$\langle \Delta p \rangle$	$\sigma_{\Delta p}$
587727178986356823	00:00:00.41	−10:22:25.7	0.543	0.0	0.011	0.0090	0.0	0.0	0.0
587727227300741210	00:00:00.74	−09:13:20.2	0.458	0.0	0.203	0.115	0.267	0.199	0.112
587727225153257596	00:00:01.03	−10:56:48.0	0.811	0.046	0.367	0.192	0.2	0.174	0.09
587730774962536596	00:00:01.38	+15:30:35.3	0.348	0.0	0.0	0.0	0.0	0.0	0.0
587731186203885750	00:00:01.55	−00:05:33.3	0.83	0.0	0.302	0.122	0.053	0.055	0.026
587727180060098638	00:00:01.57	−09:29:40.3	0.799	0.0	0.233	0.127	0.103	0.073	0.044
587731187277627676	00:00:01.86	+00:43:09.3	0.852	0.0020	0.307	0.131	0.142	0.102	0.045
587727223024189605	00:00:02.00	+15:41:49.8	0.75	0.0060	0.333	0.137	0.399	0.196	0.076
587730775499407375	00:00:02.10	+15:52:54.2	0.629	0.0	0.035	0.019	0.0	0.0	0.0
587727221950382424	00:00:02.41	+14:49:19.0	0.762	0.036	0.365	0.178	0.457	0.244	0.113
587730774425665704	00:00:02.58	+15:02:28.3	0.774	0.027	0.375	0.177	0.529	0.261	0.117
587730773888794751	00:00:02.82	+14:42:55.9	0.982	0.0	0.134	0.061	0.018	0.029	0.014
588015507658768464	00:00:03.24	−01:06:46.8	0.869	0.0	0.0	0.0	0.216	0.107	0.045
587727178449485858	00:00:03.33	−10:43:16.0	0.734	0.0060	0.333	0.126	0.517	0.228	0.08
587730773351858407	00:00:03.46	+14:11:53.6	0.698	0.024	0.381	0.165	0.455	0.241	0.099
587731187277693069	00:00:04.12	+00:45:07.9	0.527	0.0	0.0	0.0	0.011	0.045	0.028
587727227837612116	00:00:04.18	−08:44:03.0	0.856	0.0	0.306	0.126	0.071	0.059	0.027
587727225153257606	00:00:04.60	−10:58:34.7	0.797	0.046	0.374	0.191	0.303	0.197	0.097
587727180596969574	00:00:04.60	−08:56:37.6	0.649	0.0	0.077	0.035	0.156	0.11	0.052
587731187277693072	00:00:04.74	+00:46:54.2	0.336	0.0	0.046	0.042	0.034	0.042	0.039
587727227300741221	00:00:05.17	−09:13:04.6	0.788	0.018	0.356	0.172	0.179	0.159	0.081
588015507658768548	00:00:05.54	−01:12:58.9	0.674	0.0	0.034	0.017	0.183	0.127	0.074
587727221413511423	00:00:05.70	+14:24:44.8	0.724	0.02	0.363	0.176	0.458	0.243	0.113
587730775499407519	00:00:06.11	+15:52:31.4	0.797	0.046	0.374	0.191	0.303	0.197	0.097
588015509806252152	00:00:06.67	+00:30:16.8	0.847	0.0	0.317	0.136	0.108	0.101	0.049
587727221413511425	00:00:06.70	+14:19:58.5	0.604	0.0	0.0	0.0	0.0	0.0	0.0
588015510343123099	00:00:07.12	+00:51:28.5	0.762	0.0080	0.351	0.147	0.132	0.11	0.05
587727220876640496	00:00:07.35	+13:54:36.6	0.752	0.011	0.357	0.154	0.235	0.158	0.071
587730775499407506	00:00:07.37	+15:51:19.2	0.503	0.0	0.204	0.12	0.322	0.214	0.128
587730775499407527	00:00:07.59	+15:54:07.4	0.688	0.022	0.361	0.174	0.538	0.272	0.125
587730775499407394	00:00:07.62	+15:50:03.2	0.167	0.0	0.0	0.0	0.0	0.043	0.046

Note. These quantities are defined in Section 3.2. The full version of this table is available from http://data.galaxyzoo.org/. A portion is shown here for guidance regarding its form and content.

expected) there is no evidence for a preferred rotation direction in the Universe, but the results suggest that humans preferentially classify spiral galaxies as anticlockwise (Land et al. 2008). They hint at a local correlation of galaxy spins at distances less than ~0.5 Mpc – the first experimental evidence for chiral correlation of spins (Slosar et al. 2009).

The disentangling of morphological and colour-based classifications allows us to study the separate dependences of morphology and colour on environment and provide evidence that the transformation of galaxies from blue to red proceeds faster than the transformation from spiral to early type (for example, Bamford et al. 2009 and Skibba et al. 2009). The importance of this division is illustrated by the sample of passive, red, spirals in Masters et al. 2010b); these are disc galaxies on the outskirts of groups and clusters of galaxies which have either exhausted their gas, or lost it through strangulation or another mechanism.

The Galaxy Zoo results can also be used to constrain the properties of dust in spiral galaxies (Masters 2010a). Schawinski et al. (2010) use Galaxy Zoo classifications to distinguish the host galaxies of AGN, finding that in the present-day Universe activity is preferentially found in low-mass early types and high-mass late types. The sample of merging galaxies has been used to show that the local fraction of mergers is between 1 and 3 per cent and to study the global properties of merging galaxies (Darg et al. 2010a,b).

Other serendipitous discoveries have been made because of the close attention given by classifiers to each image. Galaxy Zoo has brought to light several rare classes of object. 'Hanny's Voorwerp' – an unusual emission line nebula neighbouring the spiral galaxy IC 2497 has been studied in several follow-up projects (Józsa et al. 2009; Lintott et al. 2009). An unusual class of emission line galaxies (the 'peas') have been discovered – their properties are discussed by Cardamone et al. (2009) and Amorín, Pérez-Montero & Vílchez (2010).

The success of the project, both in quickly attracting large numbers of volunteers and in providing data that are useful for science, suggests that this mode of 'citizen science' may provide a valuable method of data analysis for large data sets. A follow-up project, Galaxy Zoo 2,[2] has obtained more than 60 million more detailed classifications of a subset of the Galaxy Zoo sample, and has already produced results; Masters et al. (2010c) find that the presence of a bar is strongly linked to galaxy colour, with a bulge- and bar-dominated sequence of red galaxies separated from a predominately barless blue cloud.

Classification of galaxies drawn from large *Hubble Space Telescope* surveys is now underway.[3] Two sister projects investigating transient detection[4] and merger simulations[5] are underway, and results from these projects will be reported in future papers. Data

---

[2] http://zoo2.galaxyzoo.org
[3] http://hubble.galaxyzoo.org
[4] http://supernova.galaxyzoo.org
[5] http://mergers.galaxyzoo.org

Table 5. Classification of mirrored images during bias study.

ObjID[a]	RA	Dec.	Mirrored								Mirrored 2							
			N_{vote}	E	CW	ACW	Edge	DK	MG	CS	N_{vote}	E	CW	ACW	Edge	DK	MG	CS
587727272300741210	00:00:00.74	−09:13:20.2	111	0.396	0.135	0.0090	0.405	0.054	0.0	0.55	118	0.458	0.136	0.025	0.347	0.034	0.0	0.508
587727180060098638	00:00:01.57	−09:29:40.3	121	0.876	0.0	0.017	0.033	0.066	0.0080	0.05	133	0.835	0.0	0.015	0.045	0.105	0.0	0.06
587727221950382424	00:00:02.41	+14:49:19.0	132	0.629	0.015	0.083	0.197	0.068	0.0080	0.295	120	0.625	0.0	0.142	0.208	0.017	0.0080	0.35
587731186203951111	00:00:04.44	−00:05:00.1	105	0.962	0.0	0.01	0.019	0.01	0.0	0.029	121	0.934	0.0	0.0	0.0	0.066	0.0	0.0
587731187814563978	00:00:11.97	+01:07:18.5	122	0.025	0.033	0.91	0.0080	0.0080	0.016	0.951	126	0.0080	0.024	0.905	0.0080	0.032	0.024	0.937
587727225690128575	00:00:14.09	−10:28:45.9	119	0.882	0.017	0.0080	0.067	0.025	0.0	0.092	100	0.94	0.01	0.0	0.02	0.03	0.0	0.03
587727223024189761	00:00:14.92	+15:43:42.6	114	0.368	0.0	0.175	0.404	0.035	0.018	0.579	108	0.417	0.0090	0.102	0.398	0.074	0.0	0.509
588015508732510387	00:00:16.12	−00:13:58.4	109	0.523	0.055	0.0	0.248	0.174	0.0	0.303	117	0.615	0.051	0.0	0.197	0.128	0.0090	0.248
587730773351923979	00:00:21.19	+14:10:53.7	103	0.282	0.0	0.01	0.029	0.068	0.612	0.039	126	0.206	0.0080	0.0	0.079	0.071	0.635	0.087
588015507658768569	00:00:24.16	−01:13:20.7	111	0.703	0.0090	0.018	0.054	0.09	0.126	0.081	119	0.731	0.0	0.0	0.067	0.101	0.101	0.067
587727223024189787	00:00:25.61	+15:41:28.2	105	0.781	0.01	0.0	0.029	0.181	0.0	0.038	108	0.778	0.019	0.0	0.037	0.157	0.0090	0.056
587730773888794890	00:00:38.69	+14:35:48.2	123	0.041	0.024	0.886	0.016	0.024	0.0080	0.927	116	0.043	0.0090	0.914	0.034	0.0	0.0	0.957
587727221950447853	00:00:38.70	+14:53:40.8	107	0.421	0.0090	0.0	0.495	0.028	0.047	0.505	128	0.43	0.023	0.023	0.469	0.047	0.0080	0.516
587727221413577017	00:00:43.55	+14:31:29.5	94	0.553	0.011	0.021	0.085	0.287	0.043	0.117	138	0.616	0.0070	0.014	0.094	0.261	0.0070	0.116
588015509269446865	00:00:46.32	+00:03:54.9	140	0.943	0.0	0.0	0.036	0.014	0.0070	0.036	123	0.878	0.0080	0.0	0.041	0.065	0.0080	0.049
587727177912680582	00:00:47.50	−11:06:12.7	127	0.756	0.0	0.0	0.087	0.11	0.047	0.087	113	0.823	0.027	0.0	0.0090	0.106	0.035	0.035
587727224878384226	00:00:50.19	+15:21:44.2	128	0.836	0.0	0.0	0.016	0.031	0.117	0.016	108	0.843	0.0	0.0	0.028	0.046	0.083	0.028
587727224878384242	00:00:51.41	+15:15:03.0	128	0.305	0.0	0.398	0.195	0.078	0.023	0.594	109	0.183	0.037	0.404	0.312	0.046	0.018	0.752
588015507658834049	00:00:51.75	−01:11:53.9	128	0.914	0.0080	0.0	0.031	0.047	0.0	0.039	116	0.922	0.0	0.0090	0.052	0.017	0.0	0.06
587727225690259613	00:00:52.08	−10:35:13.0	137	0.146	0.029	0.62	0.197	0.0070	0.0	0.847	120	0.092	0.025	0.75	0.133	0.0	0.0	0.908
588015507658833960	00:00:52.97	−01:10:20.5	112	0.562	0.0	0.0	0.027	0.161	0.25	0.027	127	0.472	0.0	0.0080	0.031	0.181	0.307	0.039
588015507658834052	00:00:53.51	−01:06:55.0	123	0.902	0.0080	0.033	0.033	0.024	0.0	0.073	118	0.958	0.0080	0.0	0.0080	0.025	0.0	0.017
587730775499473122	00:00:53.54	+15:54:19.1	116	0.095	0.681	0.0	0.069	0.138	0.017	0.75	116	0.121	0.629	0.026	0.043	0.112	0.069	0.698
587727223561126046	00:00:56.33	+16:05:33.7	118	0.831	0.0	0.017	0.059	0.085	0.0080	0.076	115	0.896	0.0	0.017	0.026	0.061	0.0	0.043
587727226764001349	00:01:05.80	−09:42:40.8	111	0.892	0.0	0.0090	0.018	0.081	0.0	0.027	105	0.8	0.0	0.029	0.048	0.105	0.019	0.076
587727225690259639	00:01:06.37	−10:24:00.9	134	0.037	0.791	0.03	0.112	0.0070	0.022	0.933	112	0.062	0.795	0.036	0.08	0.0090	0.018	0.911
587730774962602228	00:01:10.17	+15:27:15.3	107	0.85	0.0	0.0	0.0090	0.14	0.0	0.0090	132	0.795	0.023	0.0	0.061	0.114	0.0	0.091
587727223561191596	00:01:16.49	+16:10:57.4	119	0.748	0.0	0.0	0.101	0.151	0.0	0.101	111	0.712	0.0	0.0090	0.063	0.216	0.0	0.072
587731185130340423	00:01:17.02	−01:01:58.2	125	0.872	0.0080	0.0080	0.048	0.064	0.0	0.064	119	0.79	0.0080	0.0080	0.059	0.134	0.0	0.076
587727178986487929	00:01:26.64	−10:11:51.9	115	0.8	0.0090	0.0	0.061	0.087	0.043	0.07	117	0.829	0.0090	0.0090	0.077	0.06	0.017	0.094
587727225690325075	00:01:31.48	−10:28:54.5	107	0.888	0.0090	0.0	0.019	0.084	0.0	0.028	111	0.865	0.0	0.0	0.018	0.117	0.0	0.018

Note. Classifications of galaxies during the bias study. Galaxies were shown mirrored about the vertical and diagonal axes ('Mirrored' and 'Mirrored 2'). For each transformation we provide the total number of votes (N_{vote}) and vote fractions categories as defined in the comments for Table 2. The full version of this table is available from http://data.galaxyzoo.org/.
[a] SDSS ID. This table includes all objects included in the Galaxy Zoo bias study sample, as described in Section 2.1.

Table 6. Classification of monochrome images during bias study.

ObjID[a]	RA	Dec.	N_{vote}	Monochrome E	CW	ACW	Edge	DK	MG	CS
587727227300741210	00:00:00.74	−09:13:20.2	108	0.565	0.019	0.083	0.278	0.056	0.0	0.38
587727180060098638	00:00:01.57	−09:29:40.3	123	0.854	0.0080	0.016	0.057	0.065	0.0	0.081
587727221950382424	00:00:02.41	+14:49:19.0	137	0.467	0.117	0.029	0.321	0.066	0.0	0.467
587731186203951111	00:00:04.44	−00:05:00.1	115	0.957	0.0	0.0	0.017	0.026	0.0	0.017
587731187814563978	00:00:11.97	+01:07:18.5	120	0.033	0.883	0.025	0.0080	0.025	0.025	0.917
587727225690128575	00:00:14.09	−10:28:45.9	108	0.907	0.0090	0.0	0.028	0.046	0.0090	0.037
587727223024189761	00:00:14.92	+15:43:42.6	115	0.27	0.113	0.0	0.539	0.078	0.0	0.652
588015508732510387	00:00:16.12	−00:13:58.4	111	0.649	0.0090	0.099	0.108	0.126	0.0090	0.216
587730773351923979	00:00:21.19	+14:10:53.7	119	0.168	0.017	0.0	0.101	0.067	0.647	0.118
588015507658768569	00:00:24.16	−01:13:20.7	117	0.598	0.06	0.0	0.094	0.197	0.051	0.154
587727223024189787	00:00:25.61	+15:41:28.2	130	0.654	0.0	0.015	0.069	0.262	0.0	0.085
587730773888794890	00:00:38.69	+14:35:48.2	97	0.041	0.918	0.01	0.0	0.021	0.01	0.928
587727221950447853	00:00:38.70	+14:53:40.8	119	0.294	0.0080	0.017	0.613	0.042	0.025	0.639
587727221413577017	00:00:43.55	+14:31:29.5	112	0.679	0.0	0.0090	0.062	0.214	0.036	0.071
588015509269446865	00:00:46.32	+00:03:54.9	128	0.891	0.016	0.0	0.047	0.0080	0.039	0.062
587727177912680582	00:00:47.50	−11:06:12.7	113	0.743	0.0	0.018	0.071	0.08	0.088	0.088
587727222487384226	00:00:50.19	+15:21:44.2	104	0.808	0.0	0.01	0.01	0.048	0.125	0.019
587727222487384242	00:00:51.41	+15:15:03.0	117	0.487	0.248	0.0090	0.171	0.077	0.0090	0.427
588015507658834049	00:00:51.75	−01:11:53.9	121	0.868	0.0080	0.017	0.041	0.066	0.0	0.066
587727225690259613	00:00:52.08	−10:35:13.0	120	0.242	0.592	0.017	0.117	0.033	0.0	0.725
588015507658833960	00:00:52.97	−01:10:20.5	114	0.395	0.026	0.0	0.088	0.228	0.263	0.114
588015507658834052	00:00:53.51	−01:06:55.0	98	0.98	0.01	0.0	0.01	0.0	0.0	0.02
587730775499473122	00:00:53.54	+15:54:19.1	127	0.118	0.0	0.717	0.031	0.118	0.016	0.748
587727223561126046	00:00:56.33	+16:05:33.7	96	0.771	0.021	0.01	0.042	0.156	0.0	0.073
587727226764001349	00:01:05.80	−09:42:40.8	105	0.886	0.01	0.01	0.038	0.057	0.0	0.057
587727225690259639	00:01:06.37	−10:24:00.9	118	0.059	0.017	0.831	0.068	0.0080	0.017	0.915
587730774962602228	00:01:10.17	+15:27:15.3	110	0.882	0.0	0.0	0.027	0.091	0.0	0.027
587727223561191596	00:01:16.49	+16:10:57.4	114	0.728	0.0090	0.0090	0.079	0.175	0.0	0.096
587731185130340423	00:01:17.02	−01:01:58.2	114	0.798	0.0	0.018	0.07	0.114	0.0	0.088
587727178986487929	00:01:26.64	−10:11:51.9	116	0.698	0.052	0.0090	0.078	0.129	0.034	0.138
587727225690325075	00:01:31.48	−10:28:54.5	128	0.891	0.0080	0.016	0.031	0.055	0.0	0.055

Note. Classifications of monochrome images of galaxies during the bias study. We provide the total number of votes (N_{vote}) and vote fractions in each of the categories, as defined in the comments for Table 2. The full version of this table is available from http://data.galaxyzoo.org/. A portion is shown here for guidance regarding its form and content.
[a]SDSS ID. This table includes all objects included in the Galaxy Zoo bias study sample, as described in Section 2.1.

from a third spin-off, which asked users to determine the length of the bars in barred galaxies, is now being reduced.[6] Obtaining a large number of visual classifications is not only inherently useful, but also provides a rich training set for improving automated techniques (Banerji et al. 2010); this combination of citizen science and machine learning will be essential in dealing with the data rates expected from future sky surveys, such as the Large Synoptic Survey Telescope (LSST Science Collaboration 2009). Whether used directly or to inform future surveys, Galaxy Zoo has shown that the efforts of volunteers, coordinated via the internet, can produce rich seams of science.

[6] http://www.icg.port.ac.uk/~hoyleb/bars/

Table 7. Combined votes including bias study data.

| ObjID[a] | RA | Dec. | N_{vote}[b] | $N_{vote,STD}$ | $N_{vote,MR1}$ | $N_{vote,MR2}$ | $N_{vote,MON}$ | Votes[c] | | | | | | |
								E	CW	ACW	Edge	DK	MG	CS
587727178986356823	00:00:00.41	−10:22:25.7	59	59	0	0	0	0.61	0.034	0.0	0.153	0.153	0.051	0.186
587727227300741210	00:00:00.74	−09:13:20.2	355	18	111	118	108	0.479	0.017	0.121	0.338	0.045	0.0	0.476
587727225153257596	00:00:01.03	−10:56:48.0	68	68	0	0	0	0.735	0.029	0.0	0.147	0.074	0.015	0.176
587307744256657700	00:00:01.28	+15:04:40.8	73	73	0	0	0	0.479	0.0	0.0	0.014	0.479	0.027	0.014
587307749625363596	00:00:01.38	+15:30:35.3	52	52	0	0	0	0.885	0.019	0.0	0.058	0.019	0.019	0.077
587731186203885750	00:00:01.55	−00:05:33.3	59	59	0	0	0	0.712	0.0	0.0	0.22	0.068	0.0	0.22
587727180060098638	00:00:01.57	−09:29:40.3	405	28	121	133	123	0.854	0.012	0.0070	0.042	0.081	0.0020	0.062
587727208766440877	00:00:01.86	+14:01:28.2	29	29	0	0	0	0.655	0.0	0.0	0.0	0.345	0.0	0.0
587731187277627676	00:00:01.86	+00:43:09.3	38	38	0	0	0	0.5	0.0	0.053	0.289	0.105	0.053	0.342
587727223024189605	00:00:02.00	+15:41:49.8	26	26	0	0	0	0.423	0.0	0.0	0.577	0.0	0.0	0.577
587307754994073775	00:00:02.10	+15:52:54.2	62	62	0	0	0	0.355	0.016	0.21	0.323	0.0	0.097	0.548
587727180060098742	00:00:02.15	−09:31:37.0	30	30	0	0	0	0.467	0.0	0.033	0.0	0.467	0.033	0.033
588015509806252142	00:00:02.28	+00:37:39.2	29	29	0	0	0	0.655	0.034	0.034	0.103	0.172	0.0	0.172
587727221950382424	00:00:02.41	+14:49:19.0	420	31	132	120	137	0.564	0.114	0.019	0.245	0.052	0.0050	0.379
587307744256657704	00:00:02.58	+15:02:28.3	24	24	0	0	0	0.583	0.042	0.125	0.167	0.083	0.0	0.333
587307738887947751	00:00:02.82	+14:42:55.9	26	26	0	0	0	0.654	0.077	0.0	0.077	0.192	0.0	0.154
587731187277627683	00:00:02.96	+00:43:04.8	24	24	0	0	0	0.583	0.0	0.083	0.167	0.125	0.042	0.25
588015507658768464	00:00:03.24	−01:06:46.8	57	57	0	0	0	0.474	0.088	0.0	0.263	0.175	0.0	0.351
587727178449485858	00:00:03.33	−10:43:16.0	24	24	0	0	0	0.125	0.0	0.0	0.875	0.0	0.0	0.875
587307733518584007	00:00:03.46	+14:11:53.6	64	64	0	0	0	0.625	0.016	0.016	0.25	0.078	0.016	0.281
587731187277693069	00:00:04.12	+00:45:07.9	30	30	0	0	0	0.933	0.0	0.033	0.0	0.033	0.0	0.033
587727227837612116	00:00:04.18	−08:44:03.0	37	37	0	0	0	0.73	0.0	0.081	0.135	0.054	0.0	0.216
587731186203951111	00:00:04.44	−00:05:00.1	371	30	105	121	115	0.951	0.0030	0.0	0.013	0.032	0.0	0.016
587727180596969574	00:00:04.60	−08:56:37.6	30	30	0	0	0	0.167	0.333	0.033	0.467	0.0	0.0	0.833

Note. The full version of this table is available from http://data.galaxyzoo.org/.
[a]SDSS ID. This table includes all objects in the Galaxy Zoo bias sample.
[b]Total number of votes for each object.
[c]Vote fractions for each category, as defined in the comments for Table 2.

for Nuclear Astrophysics, the Kavli Institute for Particle Astrophysics and Cosmology, the Korean Scientist Group, the Chinese Academy of Sciences (LAMOST), Los Alamos National Laboratory, the Max-Planck-Institute for Astronomy (MPIA), the Max-Planck-Institute for Astrophysics (MPA), New Mexico State University, Ohio State University, University of Pittsburgh, University of Portsmouth, Princeton University, the United States Naval Observatory and the University of Washington.

REFERENCES

Abraham R. G., van den Bergh S., Nair P., 2003, ApJ, 588, 218
Adelman-McCarthy J. K. et al., 2008, ApJS, 175, 297
Abazajian K. N. et al., 2009, ApJS, 182, 543
Amorín R. O., Pérez-Montero E., Vílchez J. M., 2010, ApJ, 715, 128
Ball N. M. et al., 2004, MNRAS, 348, 1038
Banerji M. et al., 2010, MNRAS, 406, 342
Bamford S. P. et al., 2009, MNRAS, 393, 1324
Barbieri M. et al., 2007, A&A, 476, 13
Cardamone C. et al., 2009, MNRAS, 399, 1191
Conselice C. J., 2006, MNRAS, 373, 1389
Darg D. et al., 2010a, MNRAS, 401, 1043
Darg D. et al., 2010b, MNRAS, 401, 1552
Fukugita M., Ichikawa T., Gunn J. E., Doi M., Schimasaku K., Schneider D. P., 1996, AJ, 111, 1748
Fukugita M. et al., 2007, AJ, 134, 579
Hubble, E., 1936, The Realm of the Nebulæ. Yale Univ. Press, New Haven, CT
Józsa G. I. G. et al., 2009, A&A, 500, 33
Kinney A. L., Calzetti D., Bohlin R. C., McQuade K., Storchi-Bergmann T., Schmitt H. R., 1996, ApJ, 467, 38
Lahav O. et al., 1995, Sci, 267, 859
Land K. & the Galaxy Zoo team, 2008, MNRAS, 388, 1686
Lintott C. J. et al., 2008, MNRAS, 389, 1179
Lintott C. J. et al., 2009, MNRAS, 399, 129
LSST Science Collaboration, preprint (arXiv: 0912.0201)
Masters K., 2010, MNRAS, 405, 783
Masters K. et al., 2010a, MNRAS, 404, 792
Masters K. et al., 2010b, preprint (arXiv: 1003.0449)
Mayo E., 1933, The Human Problems of an Industrial Civilization. MacMillian, New York, Ch. 3
Mendez B. et al., 2008, in Garmany C., Gibbs M., Moody J. W., eds, ASP Conf. Ser. Vol. 389, EPO and a Changing World: Creating Linkages and Expanding Partnerships. Astron. Soc. Pac., San Francisco, p. 219
Nair P. B., Abraham R. G., 2010, ApJS, 186, 427
Nieto-Santisteban M., Szalay A., Gray J., 2004, in Ochsenbein F., Allen M., Egret D., eds, ASP Conf. Ser. Vol. 314, Astronomical Data Analysis Software & Systems (ADASS) XIII. Astron. Soc. Pac., San Francisco, p. 666
Roberts M. S., Haynes M. P., 1994, ARA&A, 32, 115
Sandage A. R., 1961, The Hubble Atlas of Galaxies. Carnegie Institute of Washington, Washington, DC
Schawinski K., the Galaxy Zoo team, 2009, MNRAS, 396, 818
Schawinski K. et al., 2007, MNRAS, 382, 1415
Schawinski K. et al., 2010, ApJ, 711, 284
Skibba R. A. et al., 2009, MNRAS, 399, 966
Slosar A. et al., 2009, MNRAS, 392, 1225
Smith J. A. et al., 2002, AJ, 123, 2121
Strateva I. et al., 2001, AJ, 122, 1861
Strauss M. A. et al., 2002, AJ, 123, 1810
Szalay A. S., Gray J., Thakar A. R., Kunszt P. Z., Malik T., Raddick M. J., Stoughton C., vandenBerg J., 2002, in Proc. 2002 ACM SIGMOD Int. Conf. Management of Data, 570
de Vaucouleurs G. et al., 1991, Third Reference Catalog of Bright Galaxies. Springer-Verlag, New York
Westphal A. J. et al., 2006, AGU, Fall Meeting, abstract P52B-08
York D. G. et al., 2000, AJ, 120, 1579

This paper has been typeset from a TEX/LATEX file prepared by the author.